 DOI 10.1002/pmic.200300722 *Proteomics* 2004, *4,* 1950–1958

Functional protein microarrays for parallel characterisation of p53 mutants

Jonathan M. Boutell[1]*, Darren J. Hart[1]*, Benjamin L. J. Godber[1], Roland Z. Kozlowski[2] and Jonathan M. Blackburn[1, 3]

[1]Procognia Maidenhead, UK
[2]Department of Pharmacology, University of Bristol, Bristol, UK
[3]Department of Biotechnology, University of the Western Cape, Cape Town, South Africa

Understanding the way in which single nucleotide polymorphisms and mutations in the human genome result in individual susceptibility to disease is a major goal in the postgenomic era. Such knowledge should accelerate the development of personalised medicine in which drug treatment can specifically match an individual's genotype. High-throughput DNA sequencing is generating the initial information required, but new technologies are required that can rapidly characterise the phenotypic effects of the identified polymorphisms. For example, many thousands of allelic variants of the *p53* gene have been described and are responsible for more than 50% of cancers, however few of the protein products have been functionally characterised. Here we have quantified in parallel the effects of mutations and polymorphisms on the DNA-binding function of the p53 oncoprotein using a protein microarray, allowing their subclassification according to functional effect. Protein-protein interactions between p53 variants and (i) a regulatory oncoprotein, (ii) a regulatory kinase resulting in on-chip phosphorylation, are also described, suggesting the more general utility of this high-throughput assay format.

Received	30/5/03
Revised	28/11/03
Accepted	22/12/03

Keywords: DNA-protein / Functional proteomics / Microarray / p53 / Protein-protein

1 Introduction

In the postgenomic era, attention is turning towards the assignment of function to proteins encoded by genomes. As part of this effort, attempts are being made to describe the genetic differences between individuals that underlie phenotypic diversity and disease [1, 2]. Understanding this genetic variation will lead to more effective, personalised medicine whereby drug treatment can be tailored to the individual genotype of the patient. Commonly, genetic biomarkers such as single nucleotide polymorphisms (SNPs) are identified by DNA sequencing and measurements of their frequencies in different populations provide correlations with disease. Whilst a statistical association between a genetic marker and a phenotype can be valuable in disease prediction, defining the mechanistic effects of genetic changes will be key to understanding the molecular basis of individuality and the subsequent design of new targeted therapies.

When a genetic marker falls within a gene and changes the amino acid sequence of the encoded protein (*i.e.* a coding SNP or mutation), direct measurement of its effect, for example on catalytic efficiency or affinity, is possible. Such analyses are typically performed in a low-throughput manner and involve comparison of only a few mutant proteins with the wild-type. Obtaining this type of data with any degree of accuracy across large sets of protein variants is technically difficult, requiring isolation of many protein variants in an assayable format. We have used the protein microarray format [3–6] to perform comparative analyses of naturally occurring sequence variants of a single protein with the aim of dissecting the molecular mechanisms of function (or malfunction) that underlie natural variation and disease. The parallel, high-throughput nature of microarray experiments makes this format attractive for analysing large numbers of protein

Correspondence: Dr. Darren Hart, Procognia Ltd., The Switchback, Gardner Road, Maidenhead, SL67RJ, UK
E-mail: darren.hart@procognia.com
Fax: +44-1628-676-791

Abbreviations: BCCP, biotin carboxyl carrier protein; **CKII**, casein kinase II; **HRP**, horseradish peroxidase

* These authors contributed equally.

interactions and the uniform intra-array conditions both simplify and increase accuracy of assays. Additionally, the small volumes of ligand or reaction solution required to perform assays, typically tens to hundreds of microlitres, can provide economic advantages, for example when using expensive recombinant proteins.

We chose to study sequence variants of the p53 protein because of its importance in regulating the deleterious effects of oncogene activation, DNA damage and chemotherapeutic agents through activating DNA repair and apoptosis pathways [7, 8]. Approximately half of all human cancers lose p53 activity by mutation and more than 17 000 somatic and germline sequence mutations have been described [9, 10]. We have analysed 45 missense and nonsense germline mutations of *p53* (affecting the amino acid sequence of the protein), many of which result in an autosomal dominant disorder known as Li-Fraumeni syndrome (LFS) characterised by soft-tissue sarcomas, leukaemias, osteosarcomas, breast tumours, brain tumours and adrenocortical carcinoma [11, 12]. The majority of mutations are found within the DNA-binding domain with two present in the tetramerisation domain (Fig. 1A). We have also included the widely distributed polymorphism R72P [13, 14] and three control mutants in this analysis. Individual mutants have been characterised previously, often in the form of the isolated core domains, according to parameters such as DNA-binding function or folded state [15, 16]. Here we have used three physiologically relevant functional assays to carry out a side-by-side characterisation on this set of full-length, clinically relevant mutants using a microarray format. Our results clearly demonstrate differences in behaviour *in vitro* that may explain different functional effects of *p53* mutations and polymorphisms *in vivo*.

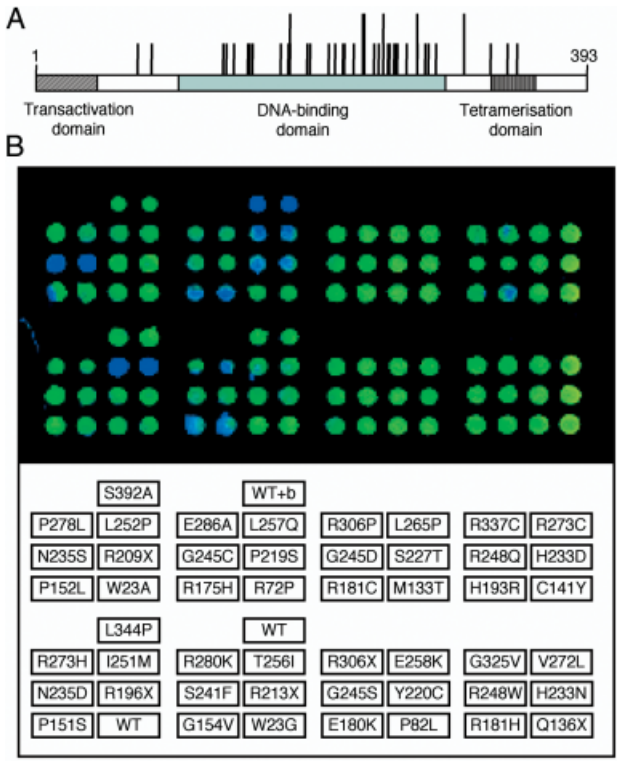

Figure 1. Microarrayed p53 variants. (A) Linear map showing domain structure of p53 and locations of the germline mutations used in this study. Presence of a longer bar indicates two separate variations. The majority of mutations are present in the DNA-binding domain (mutated amino acids 133 to 286). Outside this domain, mutant residues 72 and 82 are shown towards the *N*-terminus and 306, 325, 337 and 344 in the *C*-terminal region. Positions 23 and 392 are experimental controls and not indicated. (B) The p53 microarray probed with Cy3-labelled anti-His-tag antibody and visualised using a DNA microarray scanner. The identity of the p53 proteins are shown by the array map and comprise wild-type p53 (WT), the sequence variants (wild-type identity, amino acid position and mutation *e.g.* R175H) and wild-type co-spotted with 250 μM biotin (WT + b).

2 Materials and methods

2.1 Cloning of p53 cDNA

The wild-type *p53* gene was PCR amplified from a HeLa cell cDNA library using primers 5'-ATG GAG GAG CCG CAG TCA GAT CCT AG-3' and 5'-GAT CGC GGC CGC TCA GTC AGG CCC TTC TG-3'. The product was cloned into an *Escherichia coli* expression vector (pQE-80L; Qiagen, Valencia, CA, USA) in frame and downstream of sequences encoding six histidine residues and the BCCP domain (amino acids 74–156 of the *E. coli* AccB gene). XL1-Blue competent cells (Stratagene, La Jolla, CA, USA) were transformed and following isolation of plasmid DNA, the *p53* gene was sequence-verified and confirmed as matching Swiss-Prot entry P04637.

2.2 Construction of p53 variants

Variants of *p53* were generated by inverse PCR using the wild-type p53 expression vector as template. Phosphorylated forward primers bore the sequence variation at the 5' terminus followed by 20–24 nucleotides of *p53* sequence. Unphosphorylated reverse primers were complementary to the 20–24 nucleotides immediately before the mutated position. PCR was performed using *Pwo* polymerase (Roche, Indianapolis, IN, USA) and generated blunt ended products corresponding to the entire *p53*-containing vector. PCR products were gel purified, ligated and parental template DNA was digested with *DpnI* (New

England BioLabs, Beverly, MA, USA). XL1-Blue cells were transformed as for the original plasmid and mutant *p53* genes verified by DNA sequencing.

2.3 Expression of *p53* in *E. coli*

Individual *p53* clones were inoculated into 5 mL of Luria-Bertani medium with ampicillin at 100 μg/mL (LB amp) and shaken overnight at 250 rpm, 37°C. Four mL of each overnight culture was used to inoculate 200 mL of LB amp in shake-flasks that were incubated at 250 rpm, 37°C until an OD_{600} of 0.4 was obtained. Isopropyl-beta-D-thiogalactopyranoside (IPTG) and free biotin were added to 100 μM and 50 μM ,respectively, and proteins expressed at 30°C for 4 h. Cells were harvested by centrifugation, washed in PBS to remove excess biotin and stored as cell pellets, equivalent to 2 mL of expression culture, at −80°C. To prepare lysates, pellets were thawed on ice and resuspended in 80 μL of p53 buffer (25 mM HEPES pH 7.6, 50 mM KCl, 20% v/v glycerol, 1 mM DTT, 1 mg/mL BSA, 0.1% v/v Triton X-100) supplemented with 20 μL of 4 mg/mL lysozyme in water. The lysis mixture was incubated at 4°C for 30 min and supernatants obtained by centrifugation at 13 000 rpm, 10 min, 4°C. The mean protein concentration of the cleared lysates was 5 mg/mL as determined by Bradford assay [17] and, from SDS-PAGE and Western blot analyses, it was estimated that p53 was present at 1% of total soluble protein.

2.4 Fabrication of p53 microarrays

Cleared expression lysates were pipetted into a 384-well plate and printed onto streptavidin-coated membrane (SAM2; Promega, Madison, WI, USA) or neutravidin-derivatised, dextran-coated slides (XanTec Bioanalytics, Muenster, Germany) with a DNA microarraying robot (Genetix, New Milton, UK) refrigerated to 4°C and using 300 μm tipped pins. Each lysate was spotted in quadruplicate onto each microarray and, for microarrays printed onto SAM2 membrane, each coordinate was triple-spotted to increase protein loading. After printing, SAM2 membranes were rinsed in p53 buffer to remove unbiotinylated proteins and blocked in p53 buffer containing 5% w/v milk powder for 30 min. Following three × 5 min washes in p53 buffer, microarrays were ready for assay. Microarrays printed onto the dextran slides were washed for 5 min in p53 buffer with 50 μM biotin to block unbound neutravidin and then twice for 5 min in p53 buffer. Printed microarrays were stored in p53 buffer with 50% v/v glycerol at −20°C, and showed no loss of activity after two months.

2.5 DNA-binding assays

Oligonucleotides with the GADD45 promoter element sequence (5'-GTA CAG AAC ATG TCT AAG CAT GCT GGG GAC-3' and 5'-GTC CCC AGC ATG CTT AGA CAT GTT CTG TAC-3') were radiolabelled with γ ^{33}P-ATP (Amersham Biosciences, Little Chalfont, UK) and T4 kinase (Invitrogen, Carlsbad, CA, USA), annealed in p53 buffer and then purified using a Nucleotide Extraction column (Qiagen). The duplex oligonucleotides were quantified by UV spectrophotometry and a 2.5-fold dilution series made in p53 buffer. Five hundred μL of each dilution were incubated with microarrays at room temperature for 30 min, then washed three times for 5 min in p53 buffer to remove unbound DNA. Microarrays were then exposed to a phosphorimager plate (Fuji, Japan) overnight prior to scanning. ImaGene software (BioDiscovery, Marina del Rey, CA, USA) was used to quantify the scanned images. Four replicate values for each mutant at each DNA concentration were fitted to simple hyperbolic concentration-response curves $R = B_{max}/((K_d/L)+1)$, where R is the response in relative counts and L is the DNA concentration in nM.

2.6 Fluorescent DNA and antibody assays

Assays were performed on dextran-neutravidin slides. For the DNA-binding assays, the oligonucleotides described in Section 2.5 were synthesised with 5' Cy3 labels and annealed. Binding assays were performed with 250 nM DNA as above. For antibody binding, anti-His-tag antibody (Sigma, St. Louis, MO, USA) was labelled with Cy5 Amine Reactive Dye Pack (Amersham Biosciences) and used at a final concentration of 5 μg/mL in PBST. Binding was for 60 min followed by three × 5 min washes. In both cases, microarrays were centrifuged to remove moisture and dried; analysis of microarrays was then performed using a DNA microarray scanner (Affymetrix, Santa Clara, CA, USA).

2.7 MDM2 interaction assays

MDM2 cDNA (encoding amino acids 17–125) was amplified from a pooled cDNA library and cloned 3' to sequences encoding a His-FLAG-tag in an *Escherichia coli* expression vector. Constructs were verified by DNA sequencing and expression was confirmed by Western blot. For pull-down assays, 10 μL *MDM2*- and 10 μL p53-containing expression lysates were mixed with 20 μL anti-FLAG agarose (Sigma) in 500 μL PBS containing 300 mM NaCl, 0.1% v/v Tween 20 (PBST) and 1% w/v BSA. This was incubated at room temperature for 1 h and FLAG-bound complexes harvested by centrifugation

at 5000 rpm for 2 min. After washing in PBST, complexes were eluted in SDS-PAGE loading buffer and analysed by Western blot using a streptavidin-HRP conjugate, ECL-Plus and Hyperfilm (Amersham Biosciences). For the microarray assay, the MDM2-fusion protein was purified on Talon resin (Clontech, Palo Alto, CA, USA) and labelled with a Cy3 Amine Reactive Dye Pack. Approximately 0.75 μg of purified, Cy3-labelled MDM2 protein was incubated with p53 microarrays (printed on SAM2 membranes) in 500 μL PBST with 1% w/v BSA for 1 h at room temperature. After washing three times for 5 min in the same buffer, microarrays were dried, mounted onto glass slides and fluorescence quantified using a DNA microarray scanner (Affymetrix).

2.8 Phosphorylation assay

One unit of purified casein kinase II from rat liver (Sigma) was incubated with p53 microarrays printed on SAM2 membranes, in 400 μL p53 buffer supplemented with 15 mM $MgCl_2$ and 100 μM ATP at 30°C for 30 min. Microarrays were then washed three times for 5 min in TBST (150 mM NaCl; 10 mM Tris, pH 8.0; 0.05% v/v Tween 20). An anti-phosphoserine392 antibody (Cell Signaling Technology, Beverly, MA, USA) was added at 1/1000 dilution in 10% v/v nonfat dry milk/TBST for 1 h. After washing three times for 5 min in TBST, an anti-rabbit HRP conjugate (Cell Signaling Technology) was added at 1/2000 dilution for 1 h. After further washing, bound antibody was detected using ECLPlus and Hyperfilm.

3 Results

3.1 Microarray fabrication

Full-length *p53* cDNA was cloned into an expression plasmid downstream of sequences encoding a His-tag and residues 74–156 of the *E. coli* biotin carboxyl carrier protein (BCCP). The germline mutations were subsequently introduced into this construct by PCR mutagenesis and all clones verified by DNA sequencing and Western blot; following expression in *E. coli*, soluble, biotinylated p53 of the expected size was produced. Cleared cellular lysates from expression cultures were printed onto streptavidin-derivatised, phosphocellulose membrane or neutravidin-derivatised, dextran-coated glass slides at 4°C using a microarraying robot with 300 μm tipped, solid pins. Each spotting event delivered ~50 nL liquid containing ~10 fmol biotinylated p53 and after 30 min, microarrays were washed to remove unbiotinylated proteins. The coefficient of variation for protein loading between replicate spots was 15%. Figure 1B shows a p53 microarray on neutravidin slides, probed with a Cy3-labelled anti-His-tag antibody and demonstrating that similar amounts of each p53 variant were present. Addition of biotin to the lysate prior to arraying (spot WT + b) reduced the loading of p53, indicating that the majority of immobilisation was through the BCCP tag.

The three-dimensional nature of the membrane resulted in a higher protein-binding capacity than the coated glass slides and higher intensity signals from assays, but required mounting on glass slides for fabrication and analysis. The neutravidin-dextran coated glass slides provided simpler handling during fabrication and assays due to its compatibility with slide-based instrumentation, but bound less protein than the membrane due to the thinner layer of the surface coating.

3.2 Binding of p53 to GADD45 promoter element DNA

Replicate p53 microarrays were incubated in the presence of ^{33}P labelled duplex DNA, corresponding to the sequence of the GADD45 promoter element, at varying concentrations (Fig. 2A). The microarrays were imaged using a phosphorimager and individual spots quantified. The data were normalised against a calibration curve to compensate for the nonlinearity of this method of detection and backgrounds were subtracted. Replicate values for all mutants were plotted and analysed by nonlinear regression analysis allowing calculation of both K_d and B_{max} values (Table 1). Figure 2B shows DNA binding to wild-type p53 (high-affinity), R273H (low-affinity) and

Table 1. Summary of assay data from microarray experiments

Mutation	DNA binding		MDM2	CKII
	B_{max}/% wild-type	K_d/nM		
Wild-type	100 (90–110)	7 (5–10)	+	+
W23A	131 (119–144)	7 (5–10)	−	+
W23G	84 (74–94)	5 (3–9)	−	+
R72P	121 (110–132)	9 (7–13)	+	+
P82L	70 (63–77)	7 (5–10)	+	+
M133T	ND		+	+
Q136X	No binding		+	−
C141Y	ND		+	+
P151S	ND		+	+
P152L	31 (23–38)	18 (9–37)	+	+
G154V	ND		+	+
R175H	ND		+	+
E180K	31 (21–41)	12 (4–35)	+	+
R181C	88 (81–95)	11 (8–13)	+	+
R181H	48 (40–57)	11 (6–21)	+	+
H193R	21 (16–26)	22 (11–42)	+	+

Table 1. Continued

Mutation	DNA binding		MDM2	CKII
	B_{max}/% wild-type	K_d/ nM		
R196X	No binding		+	–
R209X	No binding		+	–
R213X	No binding		+	–
P219S	21 (14–30)	10 (3–33)	+	+
Y220C	ND		+	+
S227T	101 (94–110)	7 (5–9)	+	+
H233N	60 (52–68)	5 (3–8)	+	+
H233D	70 (58–84)	7 (3–14)	+	+
N235D	32 (25–40)	27 (15–49)	+	+
N235S	46 (36–56)	9 (4–20)	+	+
S241F	38 (30–47)	19 (10–37)	+	+
G245C	ND		+	+
G245S	44 (38–51)	11 (7–18)	+	+
G245D	ND		+	+
R248W	107 (95–120)	12 (8–17)	+	+
R248Q	85 (77–95)	17 (12–23)	+	+
I251M	ND		+	+
L252P	22 (12–32)	16 (4–63)	+	+
T256I	32 (22–41)	14 (6–34)	+	+
L257Q	26 (19–35)	17 (7–44)	+	+
E258K	ND		+	+
L265P	ND		+	+
V272L	ND		+	+
R273C	70 (56–85)	20 (11–37)	+	+
R273H	59 (40–79)	54 (27–106)	+	+
P278L	ND		+	+
R280K	54 (40–70)	21 (9–46)	+	+
E286A	32 (23–41)	22 (10–46)	+	+
R306X	No binding		+	–
R306P	90 (81–100)	7 (5–11)	+	+
G325V	73 (67–79)	7 (5–10)	+	+
R337C	88 (80–95)	6 (4–8)	+	+
L344P	No binding		+	–
S392A	121 (107–136)	10 (6–14)	+	–

The images from the DNA-binding experiment (Fig. 2) were quantified using a phosphorimager. Data were plotted and the affinity constant (K_d) and B_{max} value for each variant were determined by nonlinear regression analysis. Relative B_{max} values were calculated following normalisation of the data for protein loading and are expressed as a fraction of wild-type binding capacity. Figures in parentheses are 95% confidence intervals; ND, quantitative data not determined due to low signal intensity. Data from MDM2 interaction (Fig. 3A) and CKII phosphorylation (Fig. 4) are also summarised.

L344P (nonbinder) predicting a wild-type affinity of 7 nM. DNA binding was not observed in spots containing truncated p53 clones, *e.g.*, Q136X, effectively controlling for DNA binding by residual *E. coli* proteins remaining post-purification. A microarray was then fabricated using a streptavidin-derivatised, dextran-coated glass slide and

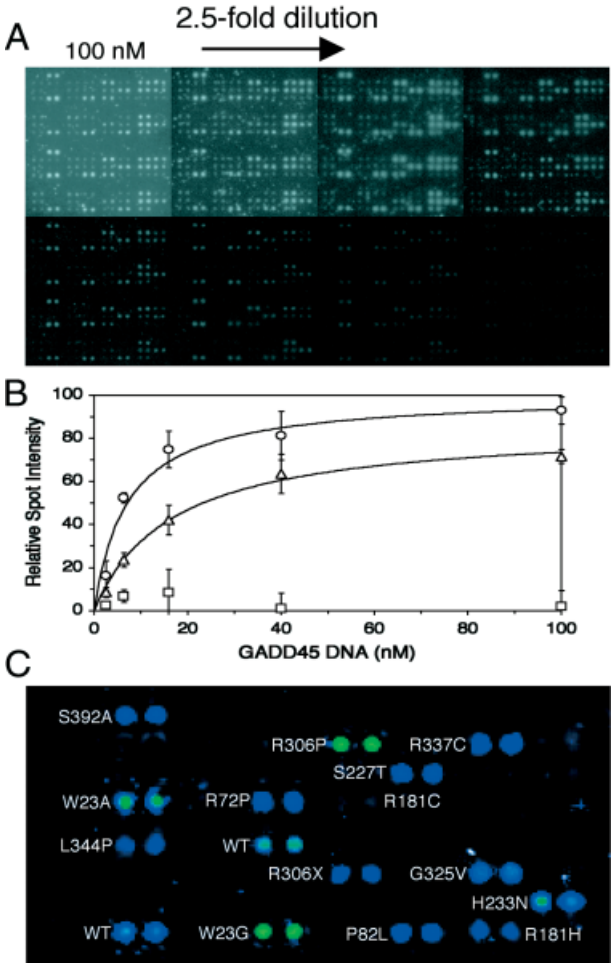

Figure 2. DNA-binding assays. (A) p53 protein microarrays probed with 2.5-fold dilution series of ^{33}P-labelled GADD45 DNA with the highest concentration at 100 nM. Bound DNA was measured with a phosphorimager after washing to remove unbound material. (B) Sample GADD45 DNA-binding curves for wild-type (○; high affinity), R273H (△; lower affinity) and L344P (□; non-binder). (C) p53 microarray printed onto a neutravidin-derivatised dextran hydrogel surface probed with Cy3-labelled GADD45 duplex oligo at 250 nM. Protein identities as in Fig. 1.

probed with Cy3-labelled GADD45-DNA under saturating ligand concentrations in a format compatible with DNA microarray analysis instrumentation (Fig. 2C). Only clones that exhibited high activity and affinity during the quantitative analysis on membranes retained DNA-binding activity on slides.

3.3 Interaction of p53 and MDM2

Bacterially expressed FLAG- and His-tagged MDM2 protein was purified and labelled with Cy3 fluorophore. Microarrays were incubated in the presence of MDM2-

Cy3 and then washed rapidly. The Cy3 fluorescence intensity of each spot was quantified using a DNA microarray scanner showing that MDM2-Cy3 bound all proteins on the microarray, though with greatly reduced binding to control mutations W23A and W23G (Fig. 3A; Table 1). Confirmation of the results in a different assay format was achieved by coincubating p53 (WT or W23A) and MDM2 *E. coli* expression lysates, after which complexes were immunoprecipitated with FLAG agarose beads. Only wild-type p53 associated with MDM2 (Fig. 3B, first lane).

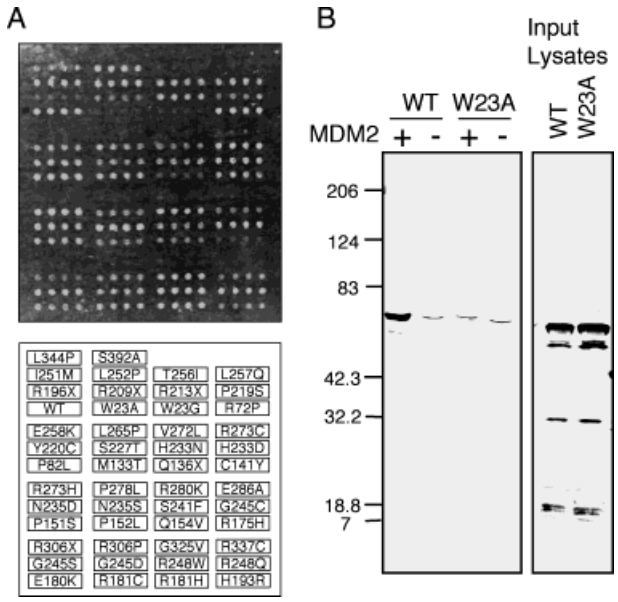

Figure 3. MDM2 interaction assays. (A) p53 microarray probed with purified Cy3-labelled MDM2 protein. Detection was performed using a DNA microarray scanner (B) Bead-based pull-down assay. FLAG-MDM2 was immunoprecipitated from a mixture of MDM2 and p53 (wild-type and W23A mutant) expression lysates. Coprecipitated, biotinylated p53 was detected by SDS-PAGE and Western blot with streptavidin-peroxidase conjugate and chemiluminescence (left blot, first lane: WT p53 + MDM2). A blot of the input *E. coli* lysates is also shown (right) demonstrating biotinylated p53 (upper band), two faint p53 degradation products and the endogenous *E. coli* BCCP (lower band of predicted mass 16.7 kDa)

3.4 On-chip phosphorylation of p53 by casein kinase II (CKII)

Microarrays were incubated in assay buffer containing ATP in the presence and absence of CKII. Phosphorylation of p53 at residue S392 was detected using an anti-phosphoserine 392 antibody and chemiluminescence (Fig. 4). In the presence of CKII, most mutants were phosphorylated and once the signal was normalised for p53 loading, it was apparent that this was to similar levels. Exceptions were the S392A negative control, mutations resulting in *C*-terminal truncations due to introduction of premature stop codons and the germline mutant L344P (summarised in Table 1).

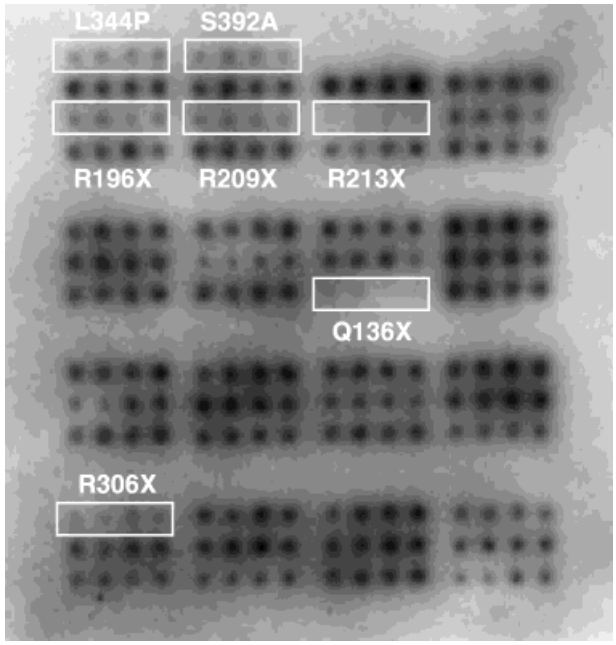

Figure 4. Phosphorylation of p53 by CK II. The p53 protein microarray was incubated with CKII and ATP. Specific phosphorylation of S392 was detected using residue-specific antiphosphoserine primary antibody with detection by secondary antibody-peroxidase conjugate and chemiluminescence. Mutations with X denote truncations due to introduction of premature stop codons and therefore lack S392. Protein identities as in Fig. 3.

4 Discussion

For many of the *p53* mutations analysed in this study little mechanistic data exists, only an association with inherited cancers. Where individual mutations have been characterised previously, comparison of data is often complicated by differences in experimental protocol. For example, the cell-based functional analysis of separated alleles in yeast (FASAY) method [18] provides information on the transactivational functionality of variants, but without detailed mechanistic information. The electrophoretic mobility shift assay (EMSA) provides quantitative information on DNA binding but is relatively low-throughput and therefore unsuitable for parallel analysis of many proteins. These issues are addressed effectively by the protein microarray format since many proteins can be assayed in the same experiment under identical conditions.

To circumvent the need for high-throughput protein purification, we exploited the high specificity and affinity of the biotin-avidin interaction to purify and immobilise proteins directly from lysates in a single step. To achieve this, p53 was fused to the compact, 80 amino acid BCCP of *E. coli* [19]. This affinity tag is biotinylated *in vivo* by endogenous biotin protein ligase (BPL) at a single, surface-exposed lysine residue located ~50Å from the *N*- and the *C*-terminus. BCCP thus provides an orientated, highly specific and essentially irreversible linkage to the surface and no significant leaching or loss of p53 activity was observed after two months of storage at −20°C in a glycerol-containing buffer. The addition of a *N*-terminal affinity tag to p53 is assumed not to affect activity and such fusions (with glutathione-*S*-transferase or hexahistidine) have been used previously in functional studies of DNA-binding, protein interactions and phosphorylation (*e.g.* [20–22]). As a general approach for fabricating protein microarrays, surface binding *via* an affinity tag may offer increased levels of protein activity since it is often observed that proteins lose activity during nonspecific adsorption or covalent cross-linking with amine-reactive chemistries. One consequence of printing crude lysates rather than prepurified proteins is that there is less control over the absolute amount of protein immobilised in each position of the microarray. We observed a two- to three-fold range in the amount of immobilised protein across the panel of mutants (Fig. 1B), probably reflecting small differences in expression levels and cell densities during growth of the individual cultures.

4.1 DNA binding

Quantitative analysis of the DNA binding data obtained from the microarrays yielded both affinities (K_d) and relative maximum binding values (B_{max}) for wild-type and mutant p53. Protein function microarrays have not been used previously in this way, therefore these data demonstrate their utility in obtaining this quality and volume of data in a parallel fashion. The alternative approach of normalising binding data for the amount of affinity-tagged protein in the spot provides a rapid means of analysing large data sets [6], however it takes into account neither the varying specific activity of the microarrayed protein nor whether the signal is recorded under saturating or subsaturating conditions. The quantitative analysis carried out here allowed the functional classification of mutants into groups according to GADD45 DNA-binding: those with wild-type affinity; those exhibiting reduced stability (low B_{max}); those with reduced affinity (higher K_d); and those showing complete loss of activity (Table 1).

Proteins with mutations outside of the DNA-binding domain generally had near wild-type affinity for DNA and include R72P, P82L, R306P and G325V. R337C is known to affect the oligomerisation state of p53 but at the assay temperature used here it is thought to be largely tetrameric [23], consistent with the affinity measured here. By contrast, total loss of binding was observed for mutations resulting in truncated proteins (Q136X, R196X, R209X and R213X where X indicates a stop codon) and mutations that monomerise the protein (L344P [24] and the tetramerisation domain deficient R306X).

Within the DNA-binding domain, we found that mutations generally reduced or abolished DNA binding. Exceptions were R181C/H, S227T and H233N/D that are solvent exposed positions, distant from the protein-DNA interface and result in wild-type binding. Mutations R248Q/W, R273C/H and R280K, present at the protein-DNA interface, exhibited low affinities with K_d values 2–7 times higher than wild-type (Table 1) consistent with either loss of specific protein-DNA interactions or steric hindrance due to the mutated residue. A previous study of DNA binding affinity of DNA contact mutants R248Q and R273H demonstrated a complete loss of interaction [15] in apparent contradiction to the reduced affinities measured here. However, this study was performed with monomeric "core" DNA binding domains. An earlier paper [25] demonstrated that, in the case of R273H, the full-length version bound DNA weakly (in accordance with our observations) due to the contributions of other contacts whilst the monomeric domain did not. This probably explains the difference between these datasets and suggests that comparisons between assay results from monomeric and tetrameric forms of p53 should be made with caution.

Many of the remaining mutants fall into a group displaying considerably reduced specific activities, apparent from very low relative B_{max} values. In some cases, residual DNA binding was with near wild-type affinity (*e.g.*, P219S, N235S) whilst in others activity was compromised to such a level that although some binding was observed, it was not quantifiable due to low signal to background ratios *e.g.*, P151S and G245C. For other mutants with low specific activities, K_d values were measurable, but with wide confidence limits *e.g.*, L252P.

Some of the mutations in this study have previously been shown, in the form of isolated core domains, to exhibit decreased thermostability and increased unfolding rates relative to the wild-type [15, 16]. Little biophysical data of this kind is available on full-length mutants but the surprisingly high thermostability exhibited by tetrameric, *E. coli*-expressed, full-length, wild-type p53 [26] suggests that some mutants may be more stable as tetramers, perhaps through interdomain contacts [27, 28], than as core

domains. It is assumed in this work that, unless the mutation specifically disrupts oligomerisation by *C*-terminal truncation or disruption of the tetramerisation domain (discussed above), the arrayed proteins are predominantly tetrameric. In addition, since p53 binds phosphocellulose [26], it is possible that the substrate used for the quantitative microarray experiments may stabilise mutants that would otherwise rapidly lose activity post immobilisation, thus permitting affinity measurements to be made for such proteins. Support for this hypothesis comes from the observation that fluorescence-based DNA-binding assays on a protein resistant, dextran-coated glass slide gave rise to broadly comparable DNA-binding profiles under saturating conditions (Fig. 2C); mutants with impaired DNA binding on phosphocellulose showed no DNA binding on the dextran surface whilst those classified as wild-type showed strong binding. It is well accepted that immobilisation can stabilise labile enzyme activities, therefore surface chemistries which exhibit high levels of protein resistance, and seem intuitively attractive for protein function microarrays, may in fact prove less optimal due to poor maintenance of the activity of less stable proteins.

4.2 MDM2 binding

The association of the MDM2 oncoprotein with the *N*-terminus of p53 and the consequent negative regulation of p53 activity through nuclear export and degradation is well understood at the mechanistic and molecular level [29] but the effect of mutation on this crucial interaction is less well understood. Although a comparison of the MDM2-p53 structure [30] with the germline mutation database [31] revealed that no mutations were present in the interface, long-range cooperative effects of the mutations might still retain the potential to disrupt MDM2 binding. Using a microarray p53-MDM2 interaction assay we observed wild-type phenotypes for all mutants except the negative control W23A/G interfacial mutants (Fig. 3A). Extrapolating from these *in vitro* data, it seems unlikely that these inherited mutations would affect the regulation of p53 activity by MDM2 *in vivo*. However, the experiment demonstrated the feasibility of the format for investigating other p53-protein interactions and offers some advantages over the commonly used two-hybrid methods [32–34], including increased throughput and control over binding conditions (*e.g.*, concentrations and buffers).

4.3 Phosphorylation

In general, many proteins are regulated by post-translational modification and in the case of p53, biological activity is strongly dependent on multisite phosphorylation by a number of kinases [35]. Despite its importance, few data exist on possible perturbations of phosphorylation patterns due to disease-related mutations. It is possible that mutations, either of the phosphorylated residue itself or in the region of the kinase interaction, might reduce phosphorylation and affect subsequent downstream events. The use of recombinant protein from *E. coli* aids the study of phosphorylation and other post-translational modifications since the protein is produced in an unmodified form. Therefore, addition of new modifications can be easily monitored [36]. The microarray-based analysis of the effect of variants on phosphorylation of the penultimate *C*-terminal residue, S392, by CKII [36] using assays based on either an antiphosphoserine 392 antibody (Fig. 4) or γ-^{33}P-ATP-based (data not shown) revealed that all p53 proteins were specifically phosphorylated except the negative control S392A, all *C*-terminal truncations and L344P. This latter mutation contains the phosphorylation site but shows a low level of modification in this assay, consistent with previous findings that it disrupts the structural integrity of p53 [23, 24] and is located at the CKII interaction site [20]. The analysis performed here is not limited to the substrate profiling of CKII: providing appropriate antiphosphoserine antibodies are available, it could be used to analyse the natural or aberrant interactions of other kinases with p53 and its mutant forms in order to elucidate the mechanisms of p53 malfunction.

5 Concluding remarks

Integrating the logistically difficult purification process with the immobilisation step during microarray fabrication has resulted in a scaleable, generic method of microarray fabrication that is capable of handling large collections of recombinant proteins. The broad spectrum of assays possible in this format may accelerate the functional characterisation of the large number of polymorphisms and mutations being identified and catalogued [1, 2]. We have performed such a study on p53, a protein representative of a wider group where sequence variants are correlated with disease from epidemiological and pathological studies, but where few data are available on their mechanistic effect. An improved understanding of how mutations disrupt protein function may lead to new therapeutic strategies involving pharmacological rescue of mutant activities, recently demonstrated using p53 as an example [16, 37, 38]. Protein microarrays may thus provide an effective format for screening compounds across panels of proteins, either for rescue of function, or for assay of efficacy across the allelic variations present between different human populations.

6 References

[1] McKusick, V. A., *Mendelian Inheritance in Man. Catalogs of Human Genes and Genetic Disorders*, Hopkins University Press, Baltimore 1998.

[2] Sachidanandam, R., Weissman, D., Schmidt, S. C., Kakol, J. M. *et al., Nature* 2001, *409*, 928–933.

[3] MacBeath, G., Schreiber, S. L., *Science* 2000, *289*, 1760–1763.

[4] Kodadek, T., *Chem. Biol.* 2001, *8*, 105–115.

[5] Zhu, H., Klemic, J. F., Chang, S., Bertone, P. *et al., Nat. Genet.* 2000, *26*, 283–289.

[6] Zhu, H., Bilgin, M., Bangham, R., Hall, D. *et al., Science* 2001, *293*, 2101–2105.

[7] Ryan, K. M., Phillips, A. C., Vousden, K. H., *Curr. Opin. Cell Biol.* 2001, *13*, 332–337.

[8] Vogelstein, B. D. L., Levine, A. J., *Nature* 2000, *408*, 307–310.

[9] Olivier, M., Eeles, R., Hollstein, M., Khan, M. A. *et al., Hum. Mutat.* 2002, *19*, 607–614.

[10] Krawczak, M., Cooper, D. N., *Trends Genet.* 1997, *13*, 121–122.

[11] Varley, J. M., Evans, D. G. R., Birch, J. M., *Br. J. Cancer* 1997, *76*, 1–14.

[12] Birch, J. M., Alston, R. D., McNally, R. J., Evans, D. G. *et al., Oncogene* 2001, *20*, 4621–4628.

[13] Beckman, G., Birgander, R., Sjalander, A., Saha, N. *et al., Hum. Hered.* 1994, *44*, 266–270.

[14] Dumont, P., Leu, J. I.-J., Della Pietra, A. C., George, D. L., Murphy, M., *Nat. Genet*. 2003, *33*, 357–365.

[15] Bullock, A. N., Henckel, J., Fersht, A. R., *Oncogene* 2000, *19*, 1245–1256.

[16] Bullock, A. N., Fersht, A. R., *Nat. Rev. Cancer* 2001, *1*, 68–76.

[17] Bradford, M. M., *Anal. Biochem.* 1976, *72*, 248–254.

[18] Ishioka, C., Frebourg, T., Yan, Y., Vidal, M. *et al., Nat. Genet.* 1993, *5*, 124–129.

[19] Chapman-Smith, A., Cronan, J. E. J., *Trends Biochem. Sci.* 1999, *24*, 359–363.

[20] Götz, C., Scholtes, P., Prowald, A., Schuster, N. *et al., Mol. Cell. Biochem.* 1999, *191*, 111–120.

[21] Buchop, S., Gibson, M. K., Wang, X. W., Wagner, P. *et al., Nucleic Acids Res.* 1997, *25*, 3868–3874.

[22] Ayed, A., Mulder, F. A. A., Yi, G. S., Lu, Y. *et al., Nat. Struct. Biol.* 2001, *8*, 756–760.

[23] Davison, T. S., Yin, P., Nie, E., Kay, C., Arrowsmith, C. H., *Oncogene* 1998, *17*, 651–656.

[24] Lomax, M. E., Barnes, D. M., Hupp, T. R., Picksley, S. M., Camplejohn, R. S., *Oncogene* 1998, *17*, 643–649.

[25] Bargettoni, J., Manfredi, J. J., Chen, X. B., Marshak, D. R., Prives, C., *Genes Dev.* 1993, *7*, 2565–2574.

[26] Nichols, N. M., Matthews, K. S., *Biochemistry* 2001, *40*, 3847–3858.

[27] Balagurumoorthy, P., Sakamoto, H., Lewis, M. S., Zambrano, N. *et al., Proc. Natl. Acad. Sci. USA* 1995, *92*, 8591–8595.

[28] Klein, C., Planker, E., Diercks, T., Kessler, H. *et al., J. Biol. Chem.* 2001, *276*, 49020–49027.

[29] Momand, J., Wu, H.-H., Dasgupta, G., *Gene* 2000, *242*, 15–29.

[30] Kussie, P. H., Gorina, S., Marechal, V., Elenbaas, B. *et al., Science* 1996, *274*, 948–953.

[31] Hernandez-Boussard, T., Rodriguez-Tome, P., Montesano, R., Hainaut, P., *Hum. Mutat.* 1999, *14*, 1–8.

[32] Li, B., Fields, S., *FASEB J.* 1993, *7*, 957–963.

[33] Iwabuchi, K., Bartel, P. L., Li, B., Marraccino, R., Fields, S., *Proc. Natl. Acad. Sci. USA* 1994, *91*, 6098–6102.

[34] Toby, G. G., Golemis, E. A., *Methods* 2001, *24*, 201–217.

[35] Appella, E., Anderson, C. W., *Eur. J. Biochem.* 2001, *268*, 2764–2772.

[36] Meek, D. W., Simon, S., Kikkawa, U., Eckhart, W., *EMBO J.* 1990, *9*, 3253–3260.

[37] Bykov, V. J., Issaeva, N., Shilov, A., Hultcrantz, M. *et al., Nat. Med.* 2002, *8*, 282–288.

[38] Foster, B. A., Coffey, H. A., Morin, M. J., Rastinejad, F., *Science* 1999, *286*, 2507–2510.

